Proceedings of the 42nd Chinese Control Conference
July 24-26, 2023, Tianjin, China

Dynamic Modeling and Maneuvering of REMUS 100 AUV: The Impact of Added Mass Coefficients

Faheem Ahmed[1], Xianbo Xiang[1,2], Guangzhao Zhou[1], Gong Xiang[1,2] Shaolong Yang[1,2]

1. School of Naval Architecture and Ocean Engineering, Huazhong University of Science and Technology, 1037, Luoyu Road, Wuhan 430074, China
E-mail: xbxiang@hust.edu.cn

2. State Key Laboratory of Intelligent Manufacturing Equipment and Technology, Huazhong University of Science and Technology, Wuhan 430074, China

Abstract: Dynamic modeling, control, and maneuvering performance of an AUV are largely reliant upon accurate prediction of hydrodynamic coefficients of an AUV maneuvering in a variety of marine environment. In this study, a large set of added mass coefficients of REMUS 100 AUV have been estimated using a different ASE technique as compared to the previously followed ASE approach. Originally, the hull and control fins be treated together in a coupled form, whereas, the current technique treats the hull and control fins separately, providing more flexibility to estimate the added mass coefficients of different parts of the AUV. A comparative study has been carried out to observe the difference between both the ASE techniques and except coupled coefficients ($Y_{\dot{r}}$=$N_{\dot{v}}$ & $M_{\dot{w}}$=$Z_{\dot{q}}$), all the other translational and rotational added mass coefficients are in good agreement. The added mass coefficients have a significant effect on the turning capabilities, speed, and stability of an AUV. Accordingly, to investigate the impact of added mass coefficients on maneuverability of an AUV, circle and spiral maneuvers were performed in a simulation environment using a nonlinear 6-DOF dynamic model. The AUV performed the maneuvers accurately showing a 5% variation in the results between the two approaches. Thus, the proposed technique is considered suitable to predict the added mass coefficients of AUVs, which require hull and control fins to be treated separately due to the arbitrary shapes and number of control fins used in bow and stern configurations. The present ASE technique is easy to implement and requires minimal computational efforts.

Key Words: Autonomous Underwater Vehicle (AUV), Analytical & Semi-Empirical (ASE), Added mass coefficient, REMUS 100 AUV, Dynamic modeling

1 Introduction

Autonomous Underwater Vehicles (AUVs) are becoming increasingly important for underwater research and exploration. Recently, the blue economy is considered an emerging concept that emphasizes the importance of sustainable utilization of ocean resources for economic growth [1–4]. AUVs are valuable tools in the research and implementation of the sustainable technologies by enabling real-time data collection, monitoring, and maintenance of offshore systems, as well as mapping the environment and remote sensing of ocean resources. These are unmanned and untethered submersible vehicles that can reach unexplored places previously inaccessible to humans. The AUVs are available in different shapes and sizes [5]. The torpedo-shaped AUVs are relatively high speed, efficient and long-distance mission vehicles with hydrodynamic fins providing steering through generating forces from forward motion. Besides various others, one of the well-known torpedo-shaped AUVs from the Remote Environmental Measuring Units (REMUS) series, the REMUS 100 AUV shown in Fig. 1, is a lightweight & compact AUV that is capable to perform a vast range of commercial & defense underwater application tasks. [6–8].

Accurate dynamic modeling and control of an AUV maneuvering in 6DOF is essentially required to perform the challenging tasks underwater [9]. To build the dynamic model of an AUV, 6-DOF equations of motion are to be solved [10]. In these equations, added mass, drag and lift forces and moment appear in terms of coefficients or derivatives and these are static, translational, rotational and acceleration derivatives. These coefficients can be estimated using several different techniques such as analytical and semi-empirical (ASE), CFD, captive or free model running testing and through system identification or machine learning approaches[5]. ASE technique is considered more direct, easy and require very less computational efforts and considered suitable for streamlined shapes to predict the hydrodynamic coefficients [11].

Besides other parameters, added mass is considered one of the important parameter in modeling underwater vehicles. When AUV moves underwater, it creates the disturbance in the fluid and accelerates the water along the direction of motion due to which additional force is observed by the vehicle [12, 13] which is termed as added mass. The added mass coefficients can have a significant impact on the maneuverability of an AUV and higher added mass can affect turning capabilities, turning radius, speed and energy consumption during the run and to asses the effect these coefficients maneuvering simulations or experiments to determine the optimal added mass coefficients are required.

Considering AUV geometry, added mass coefficients are estimated by following ASE method and AUV hull, control fins and propellers are to be treated separately. Horace Lamb [14] developed an analytical method for the prediction of added mass coefficients of a bare-hull prolate spheroid and Frederick H. Imlay (1961) [12] given the expression for 'Added mass' of a rigid body, an underwater vehicle, moving in an ideal fluid. Same have been used by many researchers to predict the coefficients of AUV [6, 15–17]. Further, to approximate the AUV hull shape, slender body theory by Newman [18] is applied. To compute the added mass coefficients for control surfaces, Humphreys and Watkinson [16] approximated the control fins with a flat plate. Similarly, Blevins [17] also provided the relationship to estimate the

added mass coefficients for a circle with fins[6].

In this study axial, cross-flow and rolling added mass coefficients for REMUS 100 AUV have been estimated following an ASE approach alternate to the method followed by Prestero [6]. A comparative study has been carried out to observe the difference between both the ASE techniques. The effect of both the approaches have been further observed by incorporating the predicted added mass coefficients in dynamic model and performing the circle and spiral maneuvers of AUV in Matlab simulation environment. To completely build the 6-DOF nonlinear dynamic model and to perform the AUV maneuvers, all the other parameters related to drag, lift and control input forces remained unchanged as listed in Appendix-B of [6].

Fig. 1: REMUS 100 AUV [8]

The paper is structured as: Followed by introduction, section 2 provides the dynamic model. In section 3, added mass coefficients are estimated. Section 4 includes, comparative study, AUV maneuvering simulations, results and discussions. Finally, conclusion and remarks are provided in section 5. The nomenclature and abbreviations used in the paper can be seen in Table 1.

2 Dynamic modeling of AUV

The vehicle dynamics are divided as Kinematics and Kinetics. Kinematics involve geometrical aspects of motion and Kinetics deal with the fluid forces and moments acting on the body. Two orthogonal coordinate systems are required to represent the AUV motion: one is inertial frame and the other is body-fixed frame as shown in Fig.2.

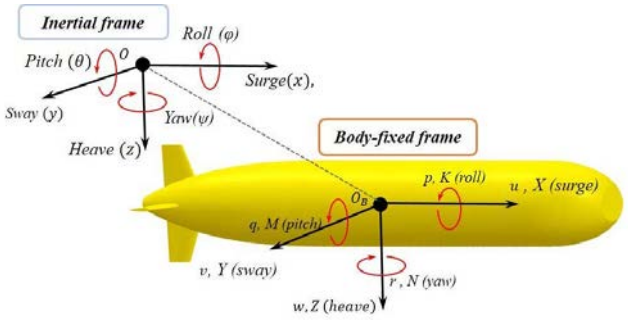

Fig. 2: Inertial and body-fixed frames

By following Fossen [19] notations, kinematics and kinetics of marine vehicle in vector form are expressed in equations (1) & (2) respectively.

$$\dot{\eta} = J_\Theta(\eta)\nu \tag{1}$$

$$M\dot{\nu}+C(\nu)\nu+D(\nu)\nu+g(\eta)=\tau \tag{2}$$

2.1 Kinematics

The positioning and orientation of an AUV moving underwater is defined in six independent coordinates. Notations for the same are given in Table 1 [19]. From equation (1), $\eta = \begin{bmatrix} p^n_{b/n} \\ \Theta_{nb} \end{bmatrix}$ and $\nu = \begin{bmatrix} v^b_{b/n} \\ w^b_{b/n} \end{bmatrix}$.

Where, $p^n_{b/n} = \begin{bmatrix} x & y & z \end{bmatrix}^\top$, $\Theta_{nb} = \begin{bmatrix} \phi & \theta & \psi \end{bmatrix}^\top$
$v^b_{b/n} = \begin{bmatrix} u & v & w \end{bmatrix}^\top$, $w^b_{b/n} = \begin{bmatrix} p & q & r \end{bmatrix}^\top$.

J_Θ is vehicle Jacobian matrix and is given by equation (3).

$$J_\Theta = \begin{bmatrix} R^n_b(\Theta_{nb}) & 0_{3\times3} \\ 0_{3\times3} & T_\Theta(\Theta_{nb}) \end{bmatrix} \tag{3}$$

Where, linear and angular velocity transformation matrices are given in equations (4) and (5) respectively.

$$R^n_b(\Theta_{nb}) = \begin{bmatrix} c\psi c\theta & -s\psi c\phi + c\psi s\theta s\phi & s\psi s\phi + c\psi c\phi s\theta \\ s\psi c\theta & c\psi c\phi + s\phi s\theta s\psi & -c\psi s\phi + s\theta s\psi c\phi \\ -s\theta & c\theta s\phi & c\theta c\phi \end{bmatrix} \tag{4}$$

$$T_\Theta(\Theta_{nb}) = \begin{bmatrix} 1 & s\phi t\theta & c\phi t\theta \\ 0 & c\phi & -s\phi \\ 0 & s\phi/c\theta & c\phi/c\theta \end{bmatrix} \tag{5}$$

In equations (4) & (5), c, s and t, represents cos, sin and tan, respectively.

2.1.1 Geometric parameters

The AUV's hull features a myring profile having length and diameter of $1.33m$ & $0.191m$ respectively. To control the AUV's maneuvering in both vertical and horizontal planes, four control fins (NACA 0012 profile), consisting of two rudders and two stern planes are positioned in a cruciform pattern at the aft of the AUV hull. Detailed information on the AUV's geometry and control fins can be found in [6].

2.2 Kinetics

Nonlinear dynamic model consisting equations of motion in vector form of an underwater vehicle, given by Fossen [19, 20] in equation (2) can be re-written as equation (6).

$$(M_{RB}+M_A)\dot{\nu}+(C_{RB}(\nu)+C_A(\nu))\nu+D(\nu)\nu+g(\eta)=\tau_c \tag{6}$$

$$\underbrace{M_{RB}\dot{\nu}+C_{RB}(\nu)\nu}_{\text{Rigid Body Forces}}+\underbrace{M_A\dot{\nu}+C_A(\nu)\nu+D(\nu)\nu}_{\text{Hydrodynamics}}+\underbrace{g(\eta)}_{\text{Hydrostatics}}=\tau_c$$

2.2.1 Rigid-body kinetics

The rigid-body equations of motion of an AUV are derived using the Newton-Euler formulation. The rigid body forces and moments are $[X, Y, Z, K, M, N]^\top$. The location of the vehicle's CG and CB in body-fixed frame are defined as $r_G = \left[x_g, y_g, z_g\right]^\top$ & $r_B = [x_b, y_b, z_b]^\top$ respectively.

Generally, the weight distribution of the AUVs are adjusted such that the CG with reference to the vehicle origin is given as $r_G = \left[0, 0, z_g\right]^\top$.

Whereas, z_g is to be kept greater than zero to achieve the roll stability of the AUV. Considering origin of the body-fixed frame at CG and AUV's top/bottom & port/starboard symmetry, the resulting inertia matrix is reduced to diagonal matrix given as $I_b = diag\{I_x, I_y, I_z\}$. Simplified form of

Table 1: Nomenclature and abbreviations

ρ	Water density	m	Mass of the AUV
CB	Center of buoyancy	CG	Center of gravity
B	Buoyancy force	W	Weight of the AUV
r_G	Location of vehicle's center of gravity	r_B	Location of vehicle's center of buoyancy
C	Vehicle Coriolis and centripetal matrix	D	Vehicle hydrodynamic lift and damping matrix
M_A	Vehicle added mass matrix	M_{RB}	Vehicle rigid body mass matrix
C_A	Vehicle added Coriolis and centripetal matrix	C_{RB}	Vehicle rigid body Coriolis and centripetal matrix
$g(\eta)$	Vector of gravitational forces	τ_c	Vector of control inputs
x, y, z	Linear positions	ϕ, θ, ψ	Euler angles (Attitude)
u, v, w	Body-fixed linear velocities	p, q, r	Body-fixed angular velocities
I_x	Mass moment of inertia of vehicle about x-axis	X, Y, Z	Control input force of the vehicle along the x, y & z-axis
I_y	Mass moment of inertia of vehicle about y-axis	K, M, N	Control input torque of the vehicle around the x, y & z-axis
I_z	Mass moment of inertia of vehicle about z-axis	m_f	Mass of the fluid
η	Position and orientation of the vehicle	ν	Velocity vector
R_b^n	Rotation matrix: vehicle frame to inertial frame	T_Θ	Translation matrix: vehicle frame to inertial frame
δ_r	Input rudder angle	δ_s	Input stern angle
x_f	Location of fin centroid from CB along x-axis	y_f	Location of fin centroid along y-axis from center axis
$X_{\dot{u}}$	Surge added mass coefficient due to surge acceleration	$X_{u\|u\|}$	Surge damping coefficient due to surge
$Y_{\dot{v}}$	Sway added mass coefficient due to sway acceleration	$Y_{v\|v\|}$	Sway damping coefficient due to sway
$Z_{\dot{w}}$	Heave added mass coefficient due to heave acceleration	$Z_{w\|w\|}$	Heave damping coefficient due to heave
$M_{\dot{w}}$	Pitch added mass coefficient due to heave acceleration	$M_{w\|w\|}$	Pitch moment damping coefficient due to heave
$N_{\dot{v}}$	Yaw added mass coefficient due to sway acceleration	$N_{v\|v\|}$	Yaw moment damping coefficient due to sway
$Y_{\dot{r}}$	Sway added mass coefficient due to yaw acceleration	$Y_{r\|r\|}$	Sway moment damping coefficient due to yaw
$Z_{\dot{q}}$	Heave added mass coefficient due to pitch acceleration	$Z_{q\|q\|}$	Heave moment damping coefficient due to pitch
$M_{\dot{q}}$	Pitch added mass coefficient due to pitch acceleration	$M_{q\|q\|}$	Pitch moment damping coefficient due to pitch
$N_{\dot{r}}$	Yaw added mass coefficient due to yaw acceleration	$N_{r\|r\|}$	Yaw moment damping coefficient due to yaw
$K_{\dot{p}}$	Rolling added mass coefficient due to roll	$K_{p\|p\|}$	Roll damping coefficient due to roll
X_{prop}	Propeller thrust	K_{prop}	Propeller torque
$Y_{uv}, Y_{ur}, Z_{uw}, Z_{uq}$	Fin lift force coefficients	$N_{uv}, N_{ur}, M_{uw}, M_{uq}$	Fin lift moment coefficients

6-DOF AUV rigid-body equations of motion in body-fixed frame are given in equation (7) [6].

$$\begin{bmatrix} X \\ Y \\ Z \\ K \\ M \\ N \end{bmatrix} = \begin{bmatrix} m\left\{\dot{u} - vr + wq - x_g\left(q^2 + r^2\right) + y_g\left(pq - \dot{r}\right) + z_g\left(pr + \dot{q}\right)\right\} \\ m\left\{\dot{v} - wp + ur - y_g\left(r^2 + p^2\right) + z_g\left(qr - \dot{p}\right) + x_g\left(qp + \dot{r}\right)\right\} \\ m\left\{\dot{w} - uq + vp - z_g\left(p^2 + q^2\right) + x_g\left(rp - \dot{q}\right) + y_g\left(rq + \dot{p}\right)\right\} \\ I_x\dot{p} + \left(I_z - I_y\right)qr + m\left\{y_g\left(\dot{w} - uq + vp\right) - z_g\left(\dot{v} - wp + ur\right)\right\} \\ I_y\dot{q} + \left(I_x - I_z\right)rp + m\left\{z_g\left(\dot{u} - vr + wq\right) - x_g\left(\dot{w} - uq + vp\right)\right\} \\ I_z\dot{r} + \left(I_y - I_x\right)pq + m\left\{x_g\left(\dot{v} - wp + ur\right) - y_g\left(\dot{u} - vr + wq\right)\right\} \end{bmatrix} \tag{7}$$

2.2.2 Hydrodynamic and hydrostatic forces

Nonlinear hydrodynamic and hydrostatic forces in form of coefficients are given in equations (8) to (14). The damping terms higher than second order are neglected.

$$\sum X = X_{HS} + X_{u|u|}u\,|u| + X_{\dot{u}}\dot{u} + X_{wq}wq + X_{qq}qq + X_{vr}vr + X_{rr}rr \tag{8}$$

$$\sum Y = Y_{HS} + Y_{v|v|}v\,|v| + Y_{r|r|}r\,|r| + Y_{\dot{v}}\dot{v} + Y_{\dot{r}}\dot{r} + Y_{ur}ur + Y_{wp}wp + Y_{pq}pq + Y_{uv}uv \tag{9}$$

$$\sum Z = Z_{HS} + Z_{w|w|}w\,|w| + Z_{q|q|}q\,|q| + Z_{\dot{w}}\dot{w} + Z_{\dot{q}}\dot{q} + Z_{uq}uq + Z_{vp}vp + Z_{rp}rp + Z_{uw}uw \tag{10}$$

$$\sum K = K_{HS} + K_{p|p|}p\,|p| + K_{\dot{p}}\dot{p} \tag{11}$$

$$\sum M = M_{HS} + M_{w|w|}w\,|w| + M_{q|q|}q\,|q| + M_{\dot{w}}\dot{w} + M_{\dot{q}}\dot{q} + M_{uq}uq + M_{vp}vp + M_{rp}rp + M_{uw}uw \tag{12}$$

$$\sum N = N_{HS} + N_{v|v|}v\,|v| + N_{r|r|}r\,|r| + N_{\dot{v}}\dot{v} + N_{\dot{r}}\dot{r} + N_{ur}ur + N_{wp}wp + N_{pq}pq + N_{uv}uv \tag{13}$$

The nonlinear hydrostatic forces and moments expressed in body-fixed frame are given in equation (14).

$$\begin{bmatrix} X_{HS} \\ Y_{HS} \\ Z_{HS} \\ K_{HS} \\ M_{HS} \\ N_{HS} \end{bmatrix} = \begin{bmatrix} -(W - B)sin(\theta) \\ (W - B)cos(\theta)sin(\phi) \\ (W - B)cos(\theta)cos(\phi) \\ -(y_gW - y_bB)cos(\theta)cos(\phi) - \left(z_gW - z_bB\right)cos(\theta)sin(\phi) \\ -(z_gW - z_bB)sin(\theta) - (x_gW - x_bB)cos(\theta)cos(\phi) \\ -(x_gW - x_bB)cos(\theta)sin(\phi) - (y_gW - y_bB)sin(\theta) \end{bmatrix} \tag{14}$$

2.2.3 Vector of control inputs

Vector of control input is given in equation (15).

$$\tau_c = \begin{bmatrix} 1 & 0 & 0 & 0 \\ 0 & Y_{uu\delta_r}u^2 & 0 & 0 \\ 0 & 0 & Z_{uu\delta_s u^2} & 0 \\ 0 & 0 & 0 & 1 \\ 0 & 0 & M_{uu\delta_s u^2} & 0 \\ 0 & N_{uu\delta_r}u^2 & 0 & 0 \end{bmatrix} \begin{bmatrix} X_{prop} \\ \delta_r \\ \delta_s \\ K_{prop} \end{bmatrix} \tag{15}$$

3 Estimation of added mass coefficients

Axial, cross-flow and rolling added mass coefficients caused due to translation and rotational maneuvers for REMUS 100 AUV, were predicted in [6] following the ASE approach and particularly for cross-flow added mass coefficients, AUV hull and control fins were treated together. Alternately, in present study hull and fins are treated separately and different estimation techniques are applied. Both the approaches are summarized in Table 2.

3.1 Axial added mass coefficient

To estimate the axial added mass coefficient resulting due to the surge velocity, the AUV hull is approximated as ellipsoid as shown in Fig. 3. The same has been calculated following the equation (16) [21].

Table 2: ASE approaches

Parameters	Prestero approach[6]	Present approach
Axial added mass coefficient	Blevins [17]	Lamb's K−factor [12, 21]
Cross-flow added mass coefficients	Newman [18] for hull & Blevins [17] for fins	Newman [18] for hull and Humphreys & Watkinson [16] for fins
Rolling added mass coefficient	Blevins [17]	Humphreys & Watkinson [16] and Gracey [22]

Fig. 3: AUV approximated to ellipsoid

$$X_{\dot{u}} = -k_1 m_f \tag{16}$$
$$\begin{cases} k_1 = -\frac{\alpha_0}{2-\alpha_0}, \;\; m_f = \frac{4}{3}\pi\rho r_1 {r_2}^2 \\ \alpha_0 = \frac{2(1-e^2)}{e^3}\left(\frac{1}{2} ln \frac{1+e}{1-e} - e\right), \;\; e = \sqrt{1-\left(\frac{r_2}{r_1}\right)^2} \end{cases}$$

Where, k_1 is Lamb's k-factor [14], m_f is mass of the fluid, e is the eccentricity of the ellipsoid, $2r_1$ and $2r_2$ are taken equivalent to the length and diameter of the vehicle respectively.

3.2 Cross flow (sway and heave) added mass coefficients

Cross flow added mass coefficients have been separately estimated for the bare-hull and fins of AUV following Newman[18] and Humphreys & Watkinson's [16] methods respectively. The cross flow added mass coefficients are estimated using equation (17).

$$\begin{cases} Y_{\dot{v}} = Z_{\dot{w}} = \underbrace{-\pi\rho \int_L R^2(x)\,dx}_{AUV\ hull} \underbrace{- 2\left(k_t \frac{\pi\rho c^2 b}{4}\right)}_{AUV\ control\ fins} \\ N_{\dot{v}} = Y_{\dot{r}} = -\pi\rho \int_L R^2(x)\; x\,dx - 2\left(k_t \frac{\pi\rho c^2 b}{4}\right) x_f \\ N_{\dot{r}} = -\pi\rho \int_L R^2(x)\; x^2 dx - 2\left\{\left(k_r \frac{\pi\rho c^3 b^2}{48}\right) + \left(k_t \frac{\pi\rho c^2 b}{4}\right) {x_f}^2\right\} \\ Y_{\dot{v}} = Z_{\dot{w}}, \;\; M_{\dot{w}} = -N_{\dot{v}}, \;\; Z_{\dot{q}} = -Y_{\dot{r}}, \;\; N_{\dot{r}} = M_{\dot{q}} \end{cases} \tag{17}$$

Where, c and b are the fin chord and span respectively. k_t is coefficient of additional mass given by Humphreys & Watkinson [16] and k_r is coefficient of additional moment of inertia presented by Gracey [22]. These coefficients are the functions of $\frac{1}{AR}$ [13, 23] as shown in Fig. 4. AR is the aspect ratio of the flat plate given as $\frac{b^2}{S}$. Where, b & S are the span and planform area of the flat plate / fins respectively.

3.3 Rolling added mass coefficient

The rotation of the AUV around the x-axis generates an added mass, which is considered insignificant for the AUV hull due to cylindrical shape, however, same is caused by the fins and considering the centroid of fin, cumulative effect due to the rotation by all four fins, rolling added mass coefficient can be estimated using the equation (18).

$$K_{\dot{p}} = -4\left\{\left(k_r \frac{\pi\rho c^3 b^2}{48}\right) + \left(k_t \frac{\pi\rho c^2 b}{4}\right) {y_f}^2\right\} \tag{18}$$

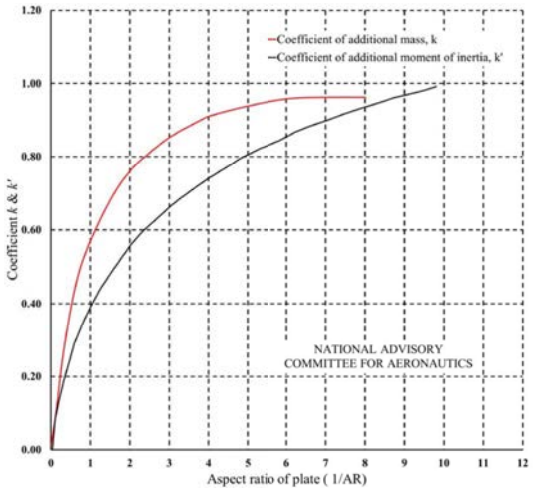

Fig. 4: Coefficient of additional mass (k_t) [16] and coefficient of additional moment of inertia (k_r) [22]

3.4 Added mass cross-terms

The hydrodynamic damping cross terms are equated with axial, cross flow and rolling added mass coefficients [6]. Same are listed in Table 3.

Table 3: Added mass cross-terms coefficients

$X_{wq} = Z_{\dot{w}}$	$X_{qq} = Z_{\dot{q}}$	$X_{vr} = -Y_{\dot{v}}$	$X_{rr} = -Y_{\dot{r}}$
$Y_{ur} = X_{\dot{u}}$	$Y_{wp} = -Z_{\dot{w}}$	$Y_{pq} = -Z_{\dot{q}}$	
$Z_{uqa} = -X_{\dot{u}}$	$Z_{vp} = Y_{\dot{v}}$	$Z_{rp} = Y_{\dot{r}}$	
$M_{uwa} = -(Z_{\dot{w}} - X_{\dot{u}})$	$M_{vp} = -Y_{\dot{r}}$	$M_{rp} = (K_{\dot{p}} - N_{\dot{r}})$	$M_{uqa} = -Z_{\dot{q}}$
$N_{uva} = -(X_{\dot{u}} - Y_{\dot{v}})$	$N_{wp} = Z_{\dot{q}}$	$N_{pq} = -(K_{\dot{p}} - M_{\dot{q}})$	$N_{ura} = Y_{\dot{r}}$

4 Results and discussions

4.1 Comparative study

Complete set of added mass coefficients and dependent cross terms estimated by Prestero [6] and following the present approach are tabulated in Table 4.

Remarks on Table 4: It has been observed from the comparative analyses that except the coupled added mass coefficients ($Y_{\dot{r}}$=$N_{\dot{v}}$ & $M_{\dot{w}}$=$Z_{\dot{q}}$) and related cross-terms coefficients, both ASE approaches for all the other translational and rotational added mass coefficients are in good agreement. However, likely cause for the large discrepancy observed for the coupled coefficients can be separate treatment of hull and fins but the same can be ascertained through some experiments. Overall combined impact of the observed variations can be investigated by performing the maneuvering of AUV in simulation and physical environment.

4.2 Maneuvering simulations

The added mass coefficients of an AUV can have a significant impact on its maneuvering performance *in general*, and turning capabilities *in particular*. Both higher and lower added mass coefficients can affect various parameters of the AUV, including vehicle speed, turning radius, turning speed, stability, and energy consumption.

To investigate the impact of added mass coefficients on the maneuverability of AUV in both horizontal and vertical planes, circle and spiral maneuvers were performed. Two

Table 4: Added mass coefficients and cross terms

Coefficients	Prestero [6] (ASE-1)	Present (ASE-2)	Percentage variations	Unit
$X_{\dot{u}}$	-0.93	-0.95	1.7%	Kg
$Y_{\dot{v}}$	-35.5	-33.2	6.4%	Kg
$Z_{\dot{w}}$	-35.5	-33.2	6.4%	Kg
$K_{\dot{p}}$	-0.0092	-0.0092	0%	Kg. m^2/rad
$M_{\dot{q}}$	-4.88	-3.8	22%	Kg. m^2/rad
$N_{\dot{r}}$	-4.88	-3.8	22%	Kg. m^2/rad
$Y_{\dot{r}}$	+1.93	+0.6	69%	Kg. m/rad
$Z_{\dot{q}}$	-1.93	-0.6	69%	Kg. m/rad
$M_{\dot{w}}$	-1.93	-0.6	69%	Kg. m
$N_{\dot{v}}$	+1.93	+0.6	69%	Kg. m
Cross terms				
X_{wq}	-35.5	-33.2	6.4%	Kg/rad
X_{qq}	-1.93	-0.6	69%	Kg. m/rad
X_{vr}	+35.5	+33.2	6.4%	Kg/rad
X_{rr}	-1.93	-0.6	69%	Kg. m/rad
Y_{ura}	-0.93	-0.95	1.7%	Kg/rad
Y_{wp}	35.5	33.2	6.4%	Kg/rad
Y_{pq}	+1.93	+0.6	69%	Kg. m/rad
Z_{uqa}	+0.93	+0.95	1.7%	Kg/rad
Z_{vp}	-35.5	-33.2	6.4%	Kg/rad
Z_{rp}	+1.93	+0.6	69%	Kg/rad
M_{uwa}	+34.6	+32.2	6.7%	Kg
M_{vp}	-1.93	-0.6	69%	Kg. m/rad
M_{rp}	+4.87	+3.8	22.2%	Kg m^2/rad^2
M_{uqa}	+1.93	+0.6	69%	Kg. m/rad
N_{uva}	-34.6	-32.2	6.7%	Kg
N_{wp}	-1.93	-0.6	69%	Kg. m/rad
N_{pq}	-4.87	-3.8	22.2%	Kg. m^2/rad^2
N_{ura}	+1.93	+0.6	69%	Kg. m/rad

sets of simulations were conducted using the added mass coefficients listed in Table 4. Simulation results achieved using the approach followed in [6] and present approach will be referred as ASE-1 and ASE-2 respectively.

4.2.1 Simulation input parameters and results

To perform the circle and spiral maneuvering simulations, input parameters such as speed and rudder/stern angles are listed in Table 5. Subscript 1 and 2 are assigned to the circle diameters (D) achieved for previous and present approaches respectively. The results are also given in Table 5.

Table 5: Simulation input parameters and result

Maneuver type	Fin angle (δ_r/δ_s)	Speed (m/s)	D_1 (m)	D_2 (m)	Δ (m)	Percentage variations
Turning-1 (Fig. 5)	$-10°$	1.54	8.72	9.22	0.51	5.4%
Turning-2 (Fig. 5)	$-5°$	1.03	9.73	10.4	0.67	6.4%
Turning-3 (Fig. 5)	$-15°$	1.03	8.01	8.42	0.41	4.9%
Spiral (Fig. 7)	$-10°/5°$	0.514	8.71	9.21	0.51	5.4 %

Remarks on Table 5 and Figures 5 & 6: Quantitative analyses show that the AUV successfully and accurately performed the circle and spiral maneuvers with an overall 5%(approx.) variation of results achieved using both the approaches. Fig. 5 shows that the results achieved using both the approaches are consistent for all the parameters such as $(u(t), x(t), y(t), \psi(t)$, etc.). To further ascertain the impact of added mass coefficients in vertical plane, field experiment results of REMUS 100 AUV, given on Page 57, Figures 7-8 of [6], have been compared with simulation results as shown in Fig. 6. The results found consistent for both the approaches.

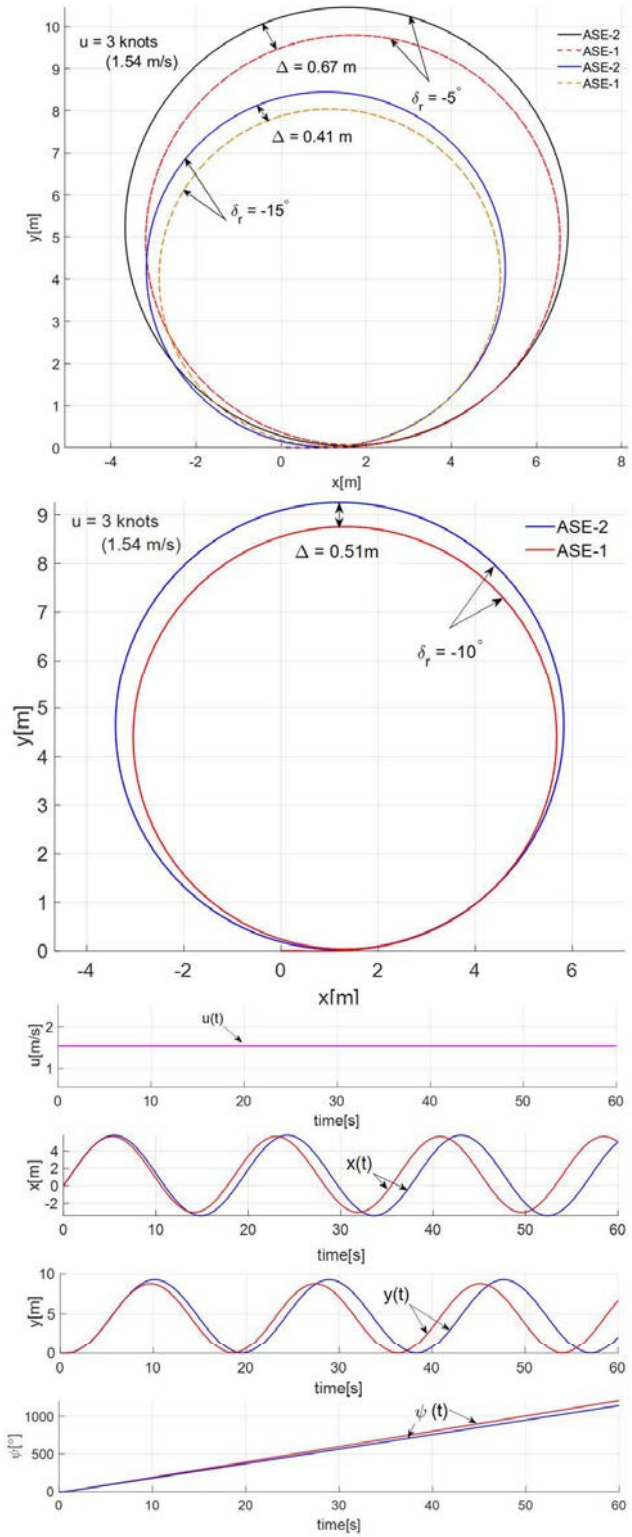

Fig. 5: Circle maneuvers

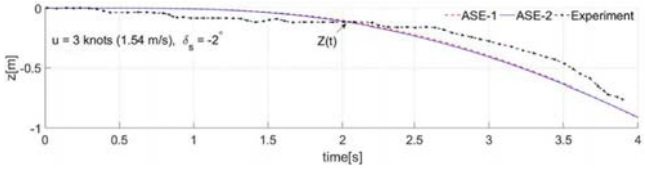

Fig. 6: Depth versus time

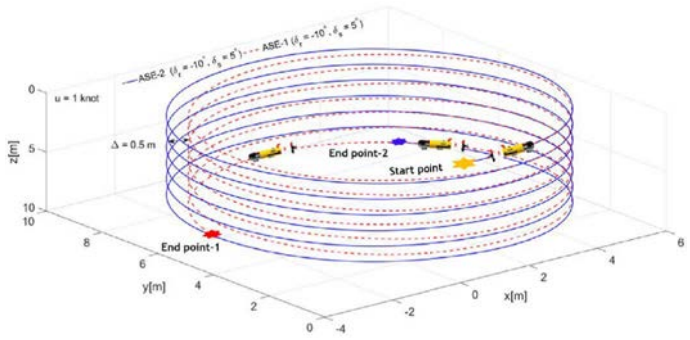

Fig. 7: Spiral maneuver

5 Conclusion and remarks

In this study, a different ASE technique has been proposed to estimate the added mass coefficients of the REMUS 100 AUV. The technique provides providing greater flexibility for estimating the added mass coefficients of different parts of the AUV. The results achieved using previous and present techniques have been compared. Except for the coupled added mass coefficients ($Y_{\dot{r}}$=$N_{\dot{v}}$ & $M_{\dot{w}}$=$Z_{\dot{q}}$), all other translational and rotational added mass coefficients showed good agreement. To investigate the impact of all the added mass coefficients on the maneuverability of vehicle in both horizontal and vertical planes, circle and spiral maneuvers were performed using the 6-DOF nonlinear dynamic model of the AUV. The AUV successfully and accurately performed the required maneuvers with an overall 5% variation in the results achieved between the two approaches. However, this small variation can be attributed to the difference in the results obtained for the yaw and sway-related added mass coefficients. Overall, maneuvering results were consistent for all the parameters such as linear and angular velocities/accelerations, yaw, and heading rates achieved using both approaches. Thus, the proposed technique is considered appropriate for predicting the added mass coefficients of AUVs, which require separate treatment of hull and control fins due to their arbitrary shapes and the number of control fins installed at bow and stern locations. The proposed ASE technique is direct, easy to implement, and requires minimal computational effort, without incurring any experimental costs.

Acknowledgement

This work is supported in part by National Natural Science Foundation of China (under Grant 52071153), in part by the Hubei Provincial Natural Science Foundation for Innovation Groups (under Grant 2021CFA026).

References

[1] W. H. Khor, H.-S. Kang, J.-W. Lim, K. Iwamoto, C. H.-H. Tang, P. S. Goh, L. K. Quen, N. M. R. B. Shaharuddin, N. Y. G. Lai, Microalgae cultivation in offshore floating photobioreactor: State-of-the-art, opportunities and challenges, Aquacultural Engineering (2022) 102269.

[2] G. Xiang, X. Xiang, X. Yu, Dynamic response of a spar-type floating wind turbine foundation with taut mooring system, Journal of Marine Science and Engineering 10 (12) (2022) 1907.

[3] P. Goh, H. Kang, A. Ismail, N. Hilal, The hybridization of thermally-driven desalination processes: The state-of-the-art and opportunities, Desalination 506 (2021) 115002.

[4] N. R. Maldar, C. Y. Ng, L. W. Ean, E. Oguz, A. Fitriadhy, H. S. Kang, A comparative study on the performance of a horizontal axis ocean current turbine considering deflector and operating depths, Sustainability 12 (8) (2020) 3333.

[5] F. Ahmed, X. Xiang, C. Jiang, G. Xiang, S. Yang, Survey on traditional and ai based estimation techniques for hydrodynamic coefficients of autonomous underwater vehicle, Ocean Engineering 268 (2023) 113300.

[6] T. T. J. Prestero, Verification of a six-degree of freedom simulation model for the remus autonomous underwater vehicle, Ph.D. thesis, Massachusetts institute of technology (2001).

[7] J. Zhang, X. Xiang, Q. Zhang, W. Li, Neural network-based adaptive trajectory tracking control of underactuated auvs with unknown asymmetrical actuator saturation and unknown dynamics, Ocean Engineering 218 (2020) 108193.

[8] T. I. Fossen, An adaptive line-of-sight (alos) guidance law for path following of aircraft and marine craft, IEEE Transactions on Control Systems Technology.

[9] X. Xiong, X. Xiang, Z. Wang, S. Yang, On dynamic coupling effects of underwater vehicle-dual-manipulator system, Ocean Engineering 258 (2022) 111699.

[10] M. Nahon, A simplified dynamics model for autonomous underwater vehicles, in: IEEE Proceedings of Symposium on Autonomous Underwater Vehicle Technology, 1996, pp. 373–379.

[11] M. E. Kepler Jr, Dynamics of a small autonomous underwater vehicle that tows a large payload, Ph.D. thesis, Virginia Tech (2018).

[12] F. H. Imlay, The complete expressions for added mass of a rigid body moving in an ideal fluid, Tech. rep., DAVID TAYLOR MODEL BASIN WASHINGTON DC (1961).

[13] J. Severholt, Generic 6-dof added mass formulation for arbitrary underwater vehicles based on existing semi-empirical methods (2017).

[14] H. Lamb, Hydrodynamics, cambridge univ, Press, (1932) 134–139.

[15] S. M. Doherty, Cross body thruster control and modeling of a body of revolution autonomous underwater vehicle, Tech. rep., NAVAL POSTGRADUATE SCHOOL MONTEREY CA (2011).

[16] D. Humphreys, K. Watkinson, Prediction of acceleration hydrodynamic coefficients for underwater vehicles from geometric parameters, Tech. rep., NAVAL COASTAL SYSTEMS LAB PANAMA CITY FL (1978).

[17] R. D. Blevins, R. Plunkett, Formulas for natural frequency and mode shape, Journal of Applied Mechanics 47 (2) (1980) 461.

[18] J. N. Newman, Marine hydrodynamics, The MIT press, 2018.

[19] T. I. Fossen, Handbook of marine craft hydrodynamics and motion control, John Wiley & Sons, 2011.

[20] T. I. Fossen, O.-E. Fjellstad, Nonlinear modelling of marine vehicles in 6 degrees of freedom, Mathematical Modelling of Systems 1 (1) (1995) 17–27.

[21] T. I. Fossen, Guidance and control of ocean vehicles, University of Trondheim, Norway, Printed by John Wiley & Sons, Chichester, England, ISBN: 0 471 94113 1, Doctors Thesis.

[22] W. Gracey, The additional-mass effect of plates as determined by experiments, Annual Report-National Advisory Committee for Aeronautics 27 (1941) 81.

[23] F. S. Malvestuto, L. J. Gale, Formulas for additional mass corrections to the moments of inertia of airplanes, Tech. rep. (1947).